chemistry proceedings

MDPI

Proceedings Paper

Exploring New Mitochondria-Targetable Theragnostic styrylBODIPYs †

Tania Mazuelo [1,2], Sergio Serrano [1], Fernando García-Garrido [1], Josué Jiménez [1], Carolina Díaz-Norambuena [1,3], Beatriz L. Maroto [1], Florencio Moreno [1], Jorge Bañuelos [3], Antonia R. Agarrabeitia [1,4], Ángeles Villanueva [5,6], Santiago de la Moya [1] and María J. Ortiz [1,*]

[1] Departamento de Química Orgánica, Facultad de Ciencias Químicas, Universidad Complutense de Madrid, Ciudad Universitaria s/n, 28040 Madrid, Spain; tmazuelo@ucm.es (T.M.); sergse02@ucm.es (S.S.); fernanga@ucm.es (F.G.-G.); cdiaz032@ikasle.ehu.eus (C.D.-N.); belora@ucm.es (B.L.M.); floren@ucm.es (F.M.); agarrabe@ucm.es (A.R.A.); santmoya@ucm.es (S.d.l.M.)
[2] Instituto Madrileño de Estudios Avanzados (IMDEA) Energía, Av. Ramón de la Sagra, 3, 28935 Móstoles, Madrid, Spain
[3] Departamento de Química Física, Facultad de Ciencia y Tecnología, Universidad del País Vasco-EHU, 48080 Bilbao, Spain; edurne.avellanal@ehu.eus (E.A.-Z.); jorge.banuelos@ehu.eus (J.B.).
[4] Sección Departamental de Química Orgánica, Facultad de Óptica y Optometría, Unversidad Complutense de Madrid, 28037 Madrid, Spain
[5] Departamento de Biología, Universidad Autónoma de Madrid, Darwin 2, 28049 Madrid, Spain; angeles.villanueva@uam.es
[6] Instituto Madrileño de Estudios Avanzados (IMDEA) Nanociencia, Ciudad Universitaria de Cantoblanco, 28049 Madrid, Spain
* Correspondence: mjortiz@quim.ucm.es; Tel.: +34-913944309 (ext. 5033)
† Presented at the 25th International Electronic Conference on Synthetic Organic Chemistry, 15–30 November 2021; Available online: https://ecsoc-25.sciforum.net/.

Citation: Mazuelo, T.; Serrano, S.; García-Garrido, F.; Jiménez, J.; Díaz-Norambuena, C.; Maroto, B.L.; Moreno, F.; Bañuelos, J.; Agarrabeitia, A.R.; Villanueva, Á.; et al. Exploring New Mitochondria-Targetable Theragnostic styrylBODIPYs. *Chem. Proc.* **2021**, *3*, x. https://doi.org/10.3390/xxxxx

Academic Editor: Julio A. Seijas

Published: 15 November 2021

Abstract: Two analogues of a previous mitochondria-targetable theragnostic styrylBODIPY have been designed, synthesized and submitted to preliminary studies in order to explore their capability to act as new theragnostic agents with absorption in the red region. The new dyes are obtained through a straightforward and low-cost synthetic protocol, and have styryl moieties bearing non-delocalized cations (trimethylammonium) attached to the BODIPY through a spacer, or directly linked. Preliminary results over of them in cell bioimaging showed internalization into HeLa cells and accumulation into mitochondria. Photodynamic therapy was also analyzed, demonstrating the viability of this red styrylBODIPY as mitochondria-targetable phototheragnostic agent.

Keywords: Red-BODIPYs; mitochondria; photodynamic therapy; bioimaging; theragnosis

1. Introduction

Boron dipyrromethenes (4-bora-3a,4a-diaza-*s*-indacene; abbreviated as BODIPY) constitute a family of organic dyes widely used in photonics due to their excellent physical and chemical properties, such as high fluorescence quantum yield, significant solubility in a wide range of organic solvents, and a great chemical versatility (known as *BODIPYs Chemistry)*, which allows finely adjusting the photophysical, chemical and biological features of these dyes [1]. An interesting modification that can be obtained through this chemistry of BODIPYs is the extension of the π-conjugation of the chromophoric core, thereby causing a bathochromic shift of the absorption and emission wavelengths towards the red edge of the visible spectrum [2].

Red-to-NIR BODIPYs are interesting due to the advantages of the red-to-NIR region (specifically, the biological window region) for biological and medical applications [3]. Thus, dyes acting in this spectral region allow using red-to-NIR light, with a deeper penetration into the tissues, among other advantages [4].

A simple way to achieve the extension of the conjugation in BODIPYs is by Knoevenagel-like condensation of BODIPYs having methyl groups at the 3/5 BODIPY positions (acidic methyls) with aromatic aldehydes, to generate the corresponding 3-styrylBODIPYs or 3,5-distyrylBODIPYs [5]. By this method, the use of functionalized aromatic aldehydes can endow the dye with additional properties such as the specific recognition of biological systems (e.g., cell organelles) [6]. In this context, red-to-NIR styryl-based BODIPYs have been successfully developed as fluorescent bioprobes and ROS (reactive oxygen species) photosensitizers for photodynamic therapy (PDT) [7,8]. Interesting PDT photosensitizers can be also tuned for conducting photo-theragnosis, which consists in performing PDT and diagnosis (by luminescence-based bioimaging) by using a single fluorescent-enough photosensitizer [9–12].

Our research group has recently demonstrated that some highly fluorescent BODIPY dyes (poor ROS photosensitizers) are able to trigger an efficient PDT action when efficiently accumulated into "sensible-to-PDT" cell organelles, such a lipid droplets (e.g., **I** and **II** in Figure 1) [13,14], or mitochondria (**III** and **IV** in Figure 1) [15]. The case of the mitochondria-targetable dyes **III** and **IV** results especially interesting, due to both chromophoric π-extension and easy synthesis (styryl-based BODIPY dyes), on the basis of using triphenylphosphonium cations to promote the accumulation into mitochondria.

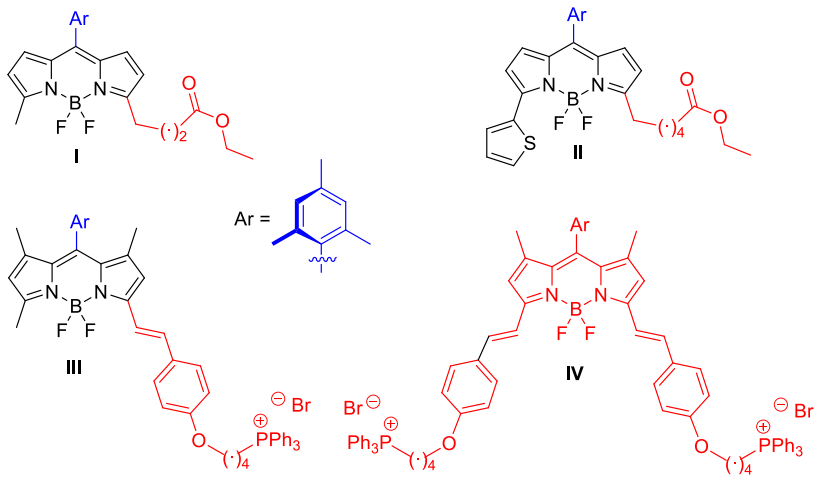

Figure 1. Structure of phototheragnostic probes for lipid droplets (**I** and **II**) and mitochondria (**III** and **IV**).

In order to cast light on the possible extension of this Knoevenagel/cation approach for the development of new, highly-fluorescent photo-theragnostic agents based on selective accumulation into mitochondria, this communication describes preliminary results on the use of different cations (specifically, trimethylammonium) and spacers.

2. Results

2.1. Synthetic Development

For our purposse, we have selected dyes **1** and **2**, which are shown in Figure 2. Compound **1** is an analogue of previous **IV**, but involving trimethylammonium cations intead of triphenylphosphonium ones. On the other hand, compound **2** is an analogue of **1,** but directly linking the key cation moiety to the chromophore, and involving meso-(p-tolyl) instead of meso-mesityl.

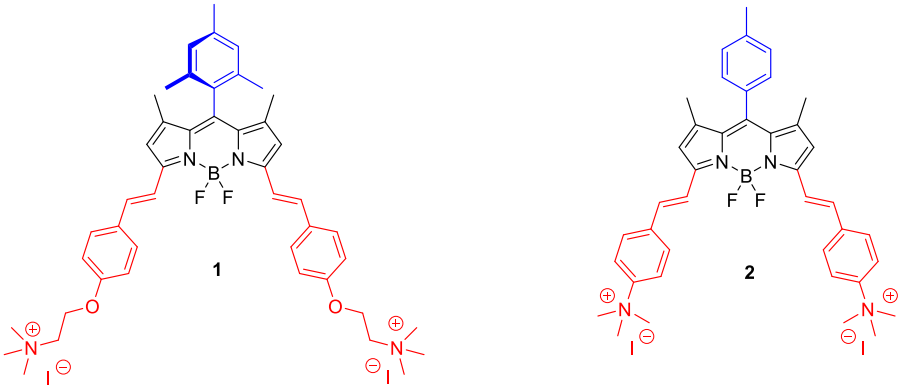

Figure 2. Selected molecular structures.

2.1.1. Synthesis of BODIPY 1

BODIPY **1** was synthesized from *meso*-mesitylBODIPY **3** [16] according to the synthetic route shown in Scheme 1. Thus, Knoevenagel-like condensation of **3** with dimethylamino-based benzaldehyde **4** [17] under microwave irradiation generatates intermediate **5** (21% yield). Finally, standard methylation of **5** with methyl iodide leads to desired **1** (78% yield).

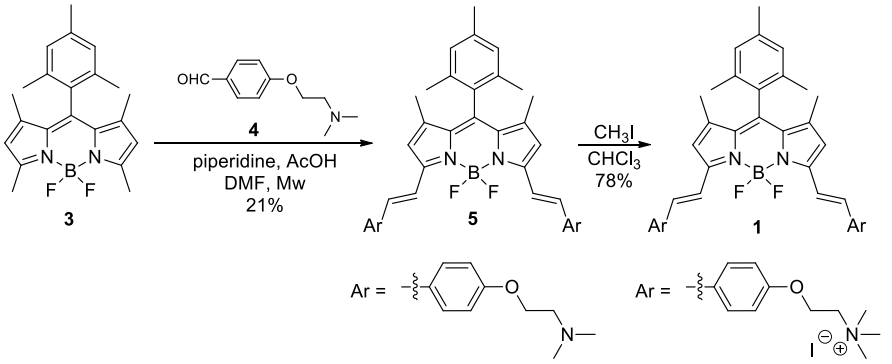

Scheme 1. Synthesis of **1**.

2.1.2. Synthesis of BODIPY 2

Analogously to that just described for BODIPY **1**, BODIPY **2** was synthesized from *meso*-(*p*-tolyl)BODIPY **6** [18] according to the synthetic route shown in Scheme 2. Thus, Knoevenagel-like condensation of **6** with commercial 4-dimethylaminobenzaldehyde under microwave irradiation to generatate intermediate **7** [19] (56% yield), followed by standard methylation with methyl iodide (quantitative yield), leads to desired **2**.

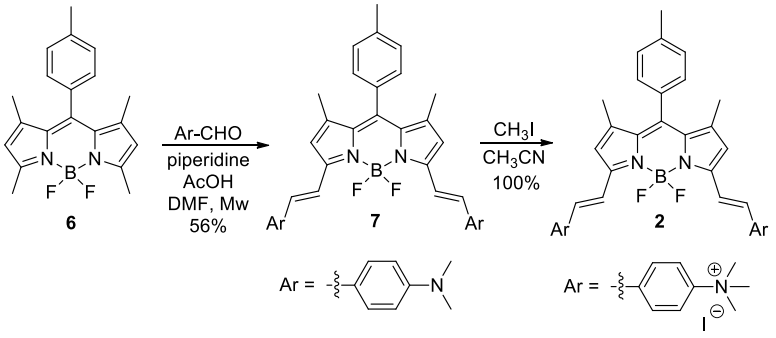

Scheme 2. Synthesis of **2**.

2.2. Photophysical Properties

The grafting of the styryl moieties at the BODIPY chromophoric positions 3 and 5 push the spectral bands of the dye deep to the red edge of the visible (around 630 and 620 nm, in ethanol for **1** and **2**, respectively, Figure 3). Indeed, the long wavelength tail of the absorption profile falls within the biological window (Figure 3). Further bathochromic shift is induced by the additional presense of the alcoxyl moiety at the styryls in the case of **1** (Table 1). These π-extended BODIPYs provide high molar absorption coefficients (around 70,000 M^{-1} cm^{-1} for **1**, Table 1), guaranteeing an optimal harvesting of the incoming red light for biomaging or photoinduced therapy. The obtained probes were characterized photophysically in EtOH solution. Accordingly, both dyes display a strong red emission (placed at around 645 and 630 nm for **1** and **2**, respectively, Figure 3), owing to their constrained geometry (reflected in low Stokes shift, lower than 300 cm^{-1}, Table 1), which minimizes undesirable non-radiative channels related with internal conversion. Specifically, dye **2** outstands by a high fluorescence efficiency (fluorescence quantum yield up to 86%, Table 1) and hence bright fluorescence images should be expected under the fluorescence microscope for this probe. Dye **1** shows a lower fluorescence efficiency (36%), although high enough for bioimaging purposses. Such different fluorescence performance could be attributed to the non-radiative deactivation channels in dye **1** related with photoinduced charge separation from the electron-rich alcoxyl-based rests to the dipyrrin, usually described as electron deficient.

Table 1. Photophysical properties of probes **1** and **2** in diluted solutions (5 μM) of H_2O and/or EtOH: absorption (λ_{ab}) and fluorescence (λ_{fl}) wavelength, molar absorption coefficient (ε_{max}), Stokes shift ($\Delta\upsilon_{St}$) and fluorescence quantum yield (φ).

Compound	Solvent	λ_{ab} (nm)	ε_{max} (10^4 M^{-1}·cm^{-1})	λ_{fl} (nm)	$\Delta\upsilon_{St}$ (cm^{-1})	φ
1	EtOH	633.0	7.09	645.0	294	0.36
2	EtOH	619.0	7.3	628.0	232	0.86
	H_2O	615.0	4.5	626.5	298	0.57

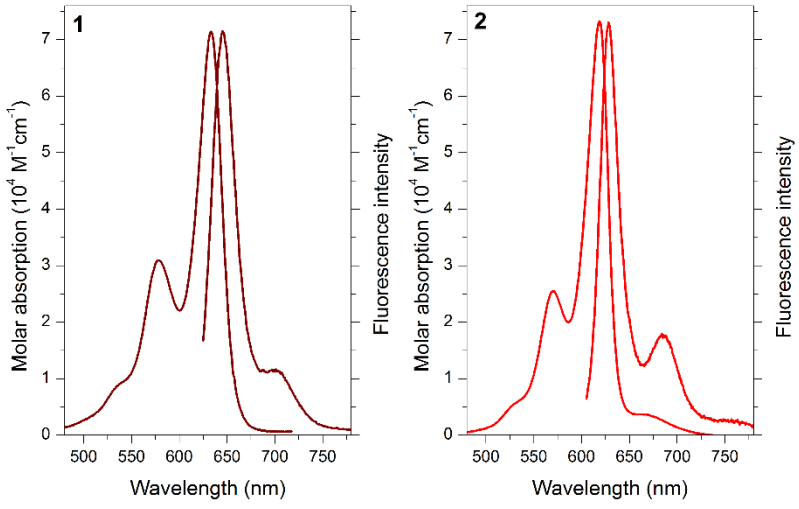

Figure 3. Absorption and normalized fluorescence spectra for probes **1** and **2** in EtOH.

Although both dyes bear cationic moieties, only the smaller one (dye **2**) is soluble in water. It is noteworthy the high fluorescence signal of dye **2** in water (57%, Table 1), and hence a similar trend should be expected in physiological media, thus avoiding the typical problems of low solubility and aggregation of the BODIPYs in aqueous media.

Therefore, both dyes absorb and emit light in a suitable region to render eficient and long lasting bioimaging. Particularly, probe **2** should behave as a better fluorescence biomarker, even in aqueous media.

2.3. Preliminary Biological Studies

Preliminary biological studies using HeLa cells and dye **1** were conducted in order to know about the possible photo-theragnostic activity of the new dyes.

2.3.1. Microscopy Studies

The conducted staining experiments, in combination with confocal microscopy, show that dye **1** is able to probe mitochondria when using an incubation time of 24 h, giving place to red or green fluorescence-based bioimages depending on the used excitation/recording microscope channels (Figure 4). On the one hand, the red bioimages display high specificity and brightness, whereas the green one is diffuse and weak. On the other hand, the specificity of the red labelling is lost when decreasing the incubation time and diffuse cytoplasmic staining can be seen in both the red and green bioimages, likely due to lack of time to complete the accumulation into the mitochondria (Figure 4A1–D1). Interestingly, phase contrast optical microscopy does not show alteration of the cell morphology, which supports lack of citotoxicity under the bioimaging-experiment conditions.

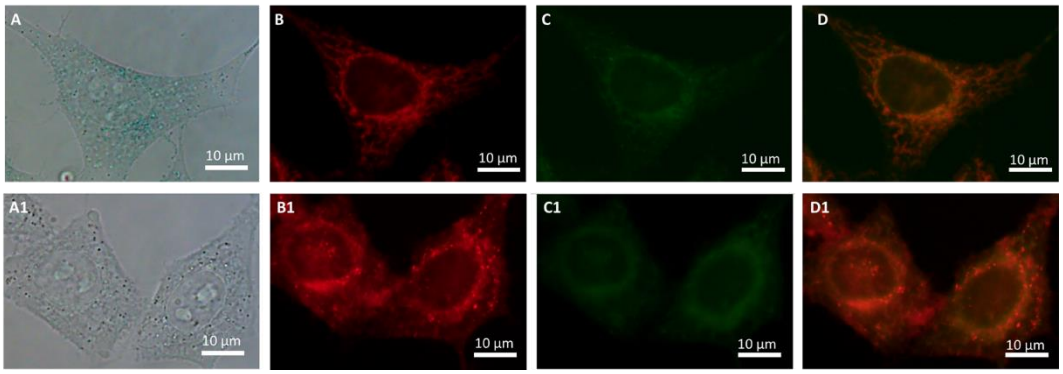

Figure 4. Images of probe **1** in HeLa cells (**A**–**D**) (5 µM, 24 h) and (**A1**–**D1**) (5 µM, 30 min) by phase contrast optical microscopy (**A**,**A1**), and by confocal microscopy using the green (**B**,**B1**) and blue (**C**,**C1**) channels, and by merging the corresponding red and green fluorescent images (**D**,**D1**).

2.3.2. Photodynamic Therapy Studies

A preliminary PDT experiment using **1** as PDT agent (5 µM; 3 h incubation; light dosis = 10.3 J/cm^2), based on the observation of key morphological changes upon the photodynamic treatment, shows that this dye is able of promoting apoptotic cell death upon ligh irradiation (Figure 5).

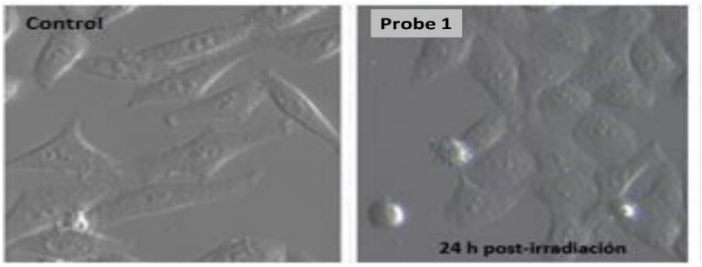

Figure 5. Image of the morphological alterations of HeLa cells incubated with probe **1** after 24 h post-irradiation.

3. Conclusions

The obtained results show that highly-accesible dye **1,** based on ammonium cation instead of triphenylphosphonium one, could serve as a new platform for the rapid development of highly-fluorescent photo-theragnostic agents based on selective accumulation into mitochondria. The results also support the capability of mitochondria to serve as sensible target for performing efficient PDT (even by using highly fluorescent photosensitizers), and envisage a promising photo-theragnostic activity for water-soluble analogue **2**. Futher experiments have been started to test this expected behavior.

4. Materials and Methods

4.1. Synthetic Procedures

General. Common solvents were dried and distilled by standard procedures. All starting materials and reagents were obtained commercially and used without further purifications. Elution flash chromatography's were conducted on silica gel (230 to 400 mesh ASTM or neutral alumina 70-290). Thin layer chromatography (TLC) was performed on silica gel plates (silica gel 60 F254, supported on aluminum). The NMR spectra were recorded at 20 °C, and the residual solvent peaks were used as internal standards. The NMR signals are given in ppm. The DEPT-135 NMR experiments were used for the assignation of the type of carbon nucleus (C, CH, CH_2, and CH_3). The FTIR spectra were recorded from neat samples using ATR technique and IR bands are given in cm^{-1}. High-resolution mass spectrometry (HRMS) was performed using ESI or MALDI-TOF.

BODIPY 5: BODIPY **3** [16] (75 mg, 0.22 mmol), **4** [17] (43 mg, 0.22 mmol), piperidine (0.07 mL, 0.66 mmol) and AcOH (0.04 mL, 0.66 mmol) were reacted in DMF (1 mL) at 120 °C for 1 h. The obtained residue was purified by flash chromatography (silica gel EtOAc/MeOH/Et_3N 79: 20: 1) to obtain **5** (33.7 mg, 21%) as a blue solid. ^{1}H NMR (300 MHz, $CDCl_3$) δ 7.61 (d, J = 16.5 Hz, 2H, 2CH), 7.56 (d, J = 8.7 Hz, 4H, 4CH), 7.20 (d, J = 16.5 Hz, 2H, 2CH), 6.96 (s, 2H, 2CH), 6.94 (d, J = 8.7 Hz, 2H, 2CH), 6.60 (s, 2H, 2CH), 4.13 (t, J = 5.7 Hz, 4H, $2CH_2$), 2.79 (t, J = 5.7 Hz, 4H, $2CH_2$), 2.38 (s, 12H, $4CH_3$), 2.34 (s, 3H, CH_3), 2.12 (s, 6H, $2CH_3$), 1.44 (s, 6H, $2CH_3$) ppm.^{13}C NMR (75 MHz, $CDCl_3$) δ 159.6 (C), 152.6 (C), 141.2 (C), 138.7 (C), 138.1 (C), 135.6 (C), 135.6 (CH), 132.5 (C), 131.4 (C), 129.8 (C), 129.1 (CH), 129.0 (CH), 117.5 (CH), 117.2 (CH), 115.0 (CH), 66.0 (CH_2), 58.2 (CH_2), 45.9 (CH_3), 21.4 (CH_3), 19.8 (CH_3), 13.8 (CH_3) ppm. FTIR ν 2925, 2856, 1600, 1537, 1490, 1252, 1201, 1166, 1111, 990 cm^{-1}. HRMS-MALDI-TOF (m/z) 716.4073 (716.4069 calcd. for $C_{44}H_{51}BF_2N_4O_2$).

BODIPY 1: To a solution of **5** (20 mg, 0.03 mmol) in $CHCl_3$ (0.5 mL), CH_3I (0.8 mL) was dropwise added, under argon atmosphere, and the reaction mixture was stirred at rt for 24 h. The solvent was removed under reduced pressure and the obtained residue was purified by flash chromatography (neutral alumina, CH_3CN/H_2O 9:1) to obtained **1** (21.1 mg, 78%) as a blue solid. ^{1}H NMR (700 MHz, acetonitrile-d_3) δ 7.63 (d, J = 8.4 Hz, 4H, 4CH), 7.54 (d, J = 16.3 Hz, 2H, 2CH), 7.43 (d, J = 16.3 Hz, 2H, 2CH), 7.07 (s, 2H, 2CH), 7.06 (d, J = 8.4 Hz, 4H, 4CH), 6.79 (s, 2H, 2CH), 4.49 (broad s, 4H, $2CH_2$), 3.79 (t, J = 4.2 Hz, 4H, $2CH_2$), 3.22 (s, 18H, $6CH_3$), 2.34 (s, 3H, CH_3), 2.09 (s, 6H, $2CH_3$), 1.46 (s, 6H, $2CH_3$) ppm. ^{13}C NMR (176 MHz, acetonitrile-d_3) δ 158.4 (C), 152.4 (C), 141.9 (C), 139.1 (C), 138.7 (C), 136.0 (CH), 135.2 (C), 132.2 (C), 130.9 (C), 130.4 (C), 128.9 (CH), 128.8 (CH), 117.7 (CH), 116.9 (CH), 115.3 (CH), 65.1 (CH_2), 62.0 (CH_2), 54.1 (CH_3), 20.3 (CH_3), 18.7 (CH_3), 12.9 (CH_3) ppm. FTIR ν 2922, 2854, 1598, 1534, 1484, 1368, 1301, 1243, 1201, 1163, 1110, 1025, 988 cm^{-1}. HRMS-MALDI-TOF (m/z) $[M\text{-}CH_3]^{+2}$ 358.2036 (758.2034 calcd. For $C_{44}H_{51}BF_2N_4O_2$).

BODIPY 2: To a solution of **7** [19] (10 mg, 0.017 mmol) in CH_3CN (1 mL), CH_3I (1 mL) was dropwise added, under argon atmosphere, and the reaction mixture was stirred at rt for 72 h. The solvent was removed under reduced pressure and the obtained residue was purified by flash chromatography (neutral alumina, CH_3CN/H_2O 9:1) to obtain **2** (14 mg, cuantitative yield) as a blue solid. ^{1}H NMR (CD_3OD, 700 MHz) δ 8.00 (d, J = 9.1 Hz, 4H), 7.89 (d, J = 9.0 Hz, 4H), 7.77 (d, J = 16.4 Hz, 2H), 7.52 (d, J = 16.4 Hz, 2H), 7.44 (d, J = 7.7 Hz, 2H), 7.28 (d, J = 7.9 Hz, 2H), 6.91 (s, 2H), 3.73 (s, 18H), 2.48 (s, 3H), 1.54 (s, 6H) ppm. ^{13}C

NMR (CD_3OD, 176 MHz) δ 153.3 (C), 148.1 (C), 144.6 (C), 142.6 (C), 141.0 (C), 140.2 (C), 135.2 (C), 134.7 (CH), 132.9 (C), 131.2 (CH), 129.9 (CH), 129.3 (CH), 122.8 (CH), 121.9 (CH), 119.6 (CH), 57.7 (CH_3), 21.4 (CH_3), 15.0 (CH_3) ppm. FTIR ν 3449, 2924, 2854, 1535, 1489, 1369, 1304, 1205, 1165 cm^{-1}. HRMS-ESI (m/z) $[M]^{+2}$ 315.1855 (315.1853 calcd. For $C_{40}H_{45}BF_2N_4$).

4.2. Photophysical Properties

Diluted solutions of the BODIPY probes (around 5×10^{-6} M) were prepared by adding the corresponding solvent (spectroscopic grade) to the residue from the adequate amount of a concentrated stock solution in ethanol, after vacuum evaporation of this solvent. UV-Vis absorption and steady-state fluorescence were recorded on a SPECORD S600 (Analytikjena) spectrophotometer and a spectrofluorimeter Fluoromax-4 (HORIBA Jobin Ybon), respectively, using 1 cm path length quartz cuvettes. Fluorescence quantum yields (φ) were calculated using commercial Nile Blue (φ = 0.27 in ethanol) as the reference.

4.3. Biological Studies

4.3.1. Fluorescence Microscopy

Fluorescence microscopy images were acquired using an Olympus BX63 automated fluorescence microscope equipped with a CoolLED pE-300 light source (CoolLed Ltd., Andover, UK) and an Olympus DP74 digital camera (Olympus, Center Valley, PA, USA).

4.3.2. Cell Cultures

HeLa cells (ATCC, CCL-2) were cultured as monolayers in Dulbecco's Modified Eagle's Medium (DMEM) supplemented with 10% (v/v) fetal calf serum 50 U/mL penicillin and 50 μg/mL streptomycin. All products were purchased from Thermo Fisher Scientific (Waltham, MA, USA) and sterilized using 0.22 μm filters (Merck Milipore, Billerica, MA, USA). Cell culture was carried out in 5% CO_2, plus 95% air atmosphere at 37 °C, and kept in a SteriCult 200 incubator (Hucoa-Erloss, Madrid, Spain). Subconfluent cell cultures seeded in 24-well plates (with or without coverslips, depending on the experiment) were used. All sterile plastics were purchased from Corning (New York, NY, USA).

4.3.3. Localization Experiments

The cells, seeded in 24-well plates with coverslips, were incubated for 30 min, and 24 h with the compound. After incubation, cells were washed in sterile PBS and the coverslip, still wet, was placed on a slide. This preparation was observed under the fluorescence microscope immediately.

4.3.4. Photodynamic Therapy Protocols

The cells were incubated for 3 h with the compounds and washed three times with sterile PBS (phosphate buffer saline). Subsequently, the cells were irradiated in complete culture medium with a Par 64 Short LED lamp (Showtec, Burgebrach Germany) with green light ($\lambda = 520 \pm 20$ nm) with a light dose of 10.3 J/cm^2. After irradiation, the cells were kept in the incubator for observation.

Author Contributions: Conceptualization and supervision, M.J.O., A.R.A. and S.d.l.M. conceived the new material; synthetic development and structure characterization, T.M., S.S., F.G.-G., J.J., F.M. and B.L.M. photophysics, J.B. and C.D.-N.; biology, Á.V. and T.M. Manuscript's final revision: M.J.O., A.R.A., J.B. and S.M. All authors have read and agreed to the published version of the manuscript.

Acknowledgments: Financial support from Spanish MINECO (CTQ2016-78454-C2-2-R, MAT2017-83856-C3-2-P and 3-P) and (PID2020-11455GB-C32 and C33), Comunidad de Madrid (S2013/MIT-2850) and Gobierno Vasco (IT912-16) is gratefully acknowledged. F.G.-G. and S.S. each thank Consejería de Educación, Juventud y Deporte de la Comunidad de Madrid and Fondo Social Europeo

for pre-doctoral contracts (CT4-21-PEJ-2020-AI-BMD-18829). C.D.-N. thanks MINECO for a pre-doctoral fellowship.

Conflicts of Interest: The authors declare no conflict of interest.

References

1. Boens, N.; Verbelen, B.; Ortiz, M.J.; Jiao, L.; Dehaen, W. Synthesis of BODIPY Dyes through Postfunctionalization of the Boron Dipyrromethene Core. *Coord. Chem. Rev.* **2019**, *399*, 213024.
2. Lu, H.; Mack, J.; Yang, Y.; Shen, Z. Structural Modification Strategies for the Rational Design of Red/NIR Region BODIPYs. *Chem. Soc. Rev.* **2014**, *43*, 4778–4823.
3. Ni, Y.; Wu, J. Far-Red and near Infrared BODIPY Dyes: Synthesis and Applications for Fluorescent pH Probes and Bio-Imaging. *Org. Biomol. Chem.* **2014**, *12*, 3774–3791.
4. Donnelly, J.L.; Offenbartl-Stiegert, D.; Marín-Beloqui, J.M.; Rizzello, L.; Battaglia, G.; Clarke, T.M.; Howorka, S.; Wilden, J.D. Exploring the Relationship between BODIPY Structure and Spectroscopic Properties to Design Fluorophores for Bioimaging. *Chem. Eur. J.* **2020**, *26*, 863–872.
5. Rurack, K.; Kollmannsberger, M.; Daub, J. Molecular Switching in the Near Infrared (NIR) with a Functionalized Boron–Dipyrromethene Dye. *Angew. Chem. Int. Ed.* **2001**, *40*, 385–387.
6. Peng, X.; Du, J.; Fan, J.; Wang, J.; Wu, Y.; Zhao, J.; Sun, S.; Xu, T. A Selective Fluorescent Sensor for Imaging Cd^{2+} in Living Cells. *J. Am. Chem. Soc.* **2007**, *129*, 1500–1501.
7. Kamkaew, A.; Lim, S.H.; Lee, H.B.; Kiew, L.V.; Chung, L.Y.; Burgess, K. BODIPY Dyes in Photodynamic Therapy. *Chem. Soc. Rev*. **2013**, *42*, 77–88.
8. Agostinis, P.; Berg, K.; Cengel, K.A.; Foster, T.H.; Girotti, A.W.; Gollnick, S.O.; Hahn, S.M.; Hamblin, M.R.; Juzeniene, A.; Kessel, D.; et al. Photodynamic Therapy of Cancer: An Update. *CA Cancer J. Clin.* **2011**, *61*, 250–281.
9. Kelkar, S.S.; Reineke, T.M. Theranostics: Combining Imaging and Therapy. *Bioconjugate Chem.* **2011**, *22*, 1879–1903.
10. Shetty, Y.; Prabhu1, P.; Prabhakar, B. Emerging vistas in theranostic medicine. *Int. J. Pharm.* **2019**, *558*, 29–42.
11. Jeyamogan, S.; Khan, N.A.; Siddiquic, R. Application and Importance of Theranostics in the Diagnosis and Treatment of Cancer. *Arch. Med. Res.* **2021**, *52*, 131–142.
12. Karaman, O.; Almammadov, T.; Emre Gedik, M.; Gunaydin, G.; Kolemen, S.; Gunbas, G. Mitochondria-Targeting Selenophene-Modified BODIPY-Based Photosensitizers for the Treatment of Hypoxic Cancer Cells. *ChemMedChem* **2019**, *14*, 1879–1886.
13. Ortiz, M.J.; Moya Cerero, S. de la; Agarrabeitia, A.R.; Prieto Castañeda, A.; García-Garrido, F.; Villanueva, A.; Tabero, A. Nuevos Compuestos de Esqueleto Boradiazaindacénico y su Uso Como Agentes Teragnósticos Basados en Acumulación en Gotas Lipídicas. Patent ES2719000, 18 May 2020.
14. Tabero, A.; García-Garrido, F.; Prieto-Castañeda, A.; Palao, E.; Agarrabeitia, A.R.; García-Moreno, I.; Villanueva, A.; Moya, S. de la; Ortiz, M.J. BODIPYs Revealing Lipid Droplets as Valuable Targets for Photodynamic Theragnosis. *Chem. Commun.* **2020**, *56*, 940–943.
15. Ortiz, M.J.; Agarrabeitia, A.R.; de la Moya, S.; Mazuelo-Santos, T.; Prieto-Castañeda, A.; Villanueva, A.; Tabero, A. Nuevos Colorants BODIPY Para Teragnosis Fotodinámica Basados en Acumulación en Mitocondrias. Patent ES2800548, 2 July 2021.
16. Fu, L.; Jiang, F.-L.; Fortin, D.; Harvey, P.D.; Liu, Y. A Reaction-Based Chromogenic and Fluorescent Chemodosimeter for Fluoride Anions. *Chem. Commun.* **2011**, *47*, 5503–5505.
17. Liew, K.-F.; Chan, K.-L.; Lee, C.-Y. Blood–Brain Barrier Permeable Anticholinesterase Aurones: Synthesis, Structure–Activity Relationship, and Drug-like Properties. *Eur. J. Med. Chem.* **2015**, *94*, 195–210.
18. Cui, A.; Peng, X.; Fan, J.; Chen, X.; Wu, Y.; Guo, B. Synthesis, Spectral Properties and Photostability of Novel Boron–Dipyrromethene Dyes. *J. Photochem. Photobiol. A* **2007**, *186*, 85–92.
19. Jiménez, J.; Díaz-Norambuena, C.; Serrano, S.; Ma, S.C.; Moreno, F.; Maroto, B.L.; Bañuelos, J.; Muller, G.; Moya, S. de la. BINO-Lated Aminostyryl BODIPYs: A Workable Organic Molecular Platform for NIR Circularly Polarized Luminescence. *Chem. Commun.* **2021**, *57*, 5750–5753.